

## Article

# EPR Spectroscopy Coupled with Spin Trapping as an Alternative Tool to Assess and Compare the Oxidative Stability of Vegetable Oils for Cosmetics

Giulia Di Prima <sup>1</sup>, Viviana De Caro <sup>1,\*</sup>, Cinzia Cardamone <sup>2</sup>, Giuseppa Oliveri <sup>2</sup> and Maria Cristina D'Oca <sup>3</sup>

<sup>1</sup> Department of Biological, Chemical and Pharmaceutical Sciences and Technologies, University of Palermo, Via Archirafi 32, 90123 Palermo, Italy; giulia.diprima@unipa.it

<sup>2</sup> Food Microbiology Area, Experimental Zooprophyllactic Institute of Sicily, Via Gino Marinuzzi 3, 90129 Palermo, Italy; cinzia.cardamone@izssicilia.it (C.C.); giuseppa.oliveri@izssicilia.it (G.O.)

<sup>3</sup> Department of Physics and Chemistry "Emilio Segrè", University of Palermo, Viale delle Scienze, Ed. 18, 90128 Palermo, Italy; mariacristina.docca@unipa.it

\* Correspondence: viviana.decaro@unipa.it; Tel.: +39-09123891926

**Abstract:** Antioxidants are the most popular active ingredients in anti-aging cosmetics as they can restore the physiological radical balance and counteract the photoaging process. Instead of adding pure compounds into the formulations, some "precious" vegetable oils could be used due to their content of tocopherols, phenols, vitamins, etc., constituting a powerful antioxidant unsaponifiable fraction. Here, electron paramagnetic resonance (EPR) spectroscopy coupled with spin trapping was proven to provide a valid method for evaluating the antioxidant properties and the oxidative resistance of vegetable oils which, following UV irradiation, produce highly reactive radical species although hardly detectable. Extra virgin olive oil, sweet almond oil, apricot kernel oil, and jojoba oil were then evaluated by using N-t-butyl- $\alpha$ -phenylnitron as a spin trapper and testing different UV irradiation times followed by incubation for 5 to 180 min at 70 °C. The EPR spectra were manipulated to obtain quantitative information useful for comparing the different tested samples. As a result, the knowledge acquired via the EPR analyses demonstrated jojoba oil as the best of the four considered oils in terms of both starting antioxidant ability and oxidative stability overtime. The obtained results confirmed the usefulness of the EPR spin trapping technique for the main proposed purpose.

**Keywords:** extra virgin olive oil; almond oil; apricot kernel oil; jojoba oil; antioxidant activity; electron paramagnetic resonance spectroscopy; spin trapping; UV irradiation; cosmetics



**Citation:** Di Prima, G.; De Caro, V.; Cardamone, C.; Oliveri, G.; D'Oca, M.C. EPR Spectroscopy Coupled with Spin Trapping as an Alternative Tool to Assess and Compare the Oxidative Stability of Vegetable Oils for Cosmetics. *Appl. Sci.* **2024**, *14*, 10766. <https://doi.org/10.3390/app142210766>

Academic Editors: Athanasia Varvaresou, Spyros Papageorgiou and Panagoula Pavlou

Received: 6 October 2024

Revised: 5 November 2024

Accepted: 18 November 2024

Published: 20 November 2024



**Copyright:** © 2024 by the authors. Licensee MDPI, Basel, Switzerland. This article is an open access article distributed under the terms and conditions of the Creative Commons Attribution (CC BY) license (<https://creativecommons.org/licenses/by/4.0/>).

## 1. Introduction

Aging is a complex and multifactorial process caused by intrinsic (chronological aging) and extrinsic factors such as stress, obesity, air pollution, smoking, and, especially, sunlight exposure (photoaging), which result in spotted and wrinkled, aged skin. While chronological aging depends on intrinsic individual factors, photoaging is the result of the unprotected exposure to solar ultraviolet (UV) radiation. The latter was also demonstrated to be implicated in various types of skin carcinomas. Although the leading causes are different, the cellular and molecular mechanisms that determine both chronological aging and photoaging share fundamental molecular pathways implicating the production of free radicals [1,2]. Anti-aging products act through different mechanisms aimed at minimizing the visible signs of aging or preventing the photoaging process. The employed active ingredients are moisturizers, emollients, sun filters, exfoliants, depigments, and antioxidants [3]. The latter are also inserted as supplements in sunscreen products together with micronutrients and DNA repair enzymes as secondary protective agents (the primary ones are the physical and chemical sun filters) to limit skin damage and provide additional anticarcinogenic protection. Vitamins C and E, zinc, and selenium and phenols are the

most representative substances [4–6]. In particular, natural phenols contribute to reducing oxidative stress, inflammation, and cellular damage both in the aged dermis and in wounded skin, also improving effectiveness when appropriately administered [7,8]

Antioxidants work on three levels to combat free radicals: (i) they inhibit the radicals' formation both before and (ii) after the sunlight-determined insult, (iii) they may also correct some sunlight-determined damages [9]. In the last few years, there has been a growing demand for “naturally derived” or “organic” products as cosmeceutical ingredients useful in the personal care and beauty. Moreover, from the perspective of a circular economy, the recycling of agri-food waste to recover functional biomolecules represents an environmental-friendly strategy to obtain sustainable cosmetic/pharmaceutical ingredients [10,11]. As a result, remarkable effort has been made to assess the efficacy of plant-derived compounds and oils as bioactive ingredients in the cosmetic industry [12]. Particularly, vegetable oils are natural-based ingredients that have gained interest as active ingredients to develop cosmeceuticals due to their UV absorbing and antioxidant properties [13]. Vegetable oils have considerable antioxidant properties through different mechanisms such as radical scavenging, due both to their unsaturated fatty acid composition and high levels of natural antioxidants, such as phenols (polyphenols and tocopherols) and carotenoids [14–17].

EPR spectroscopy is an effective technique to evaluate the antioxidant properties and compare different materials. It was used to monitor the level of radicals resulting from irradiation of pharmaceuticals and dried fruit [18] and could be effective in evaluating the amount of free radicals produced during UV exposure of vegetable oils. It is unlikely that vegetable oils form very reactive radicals that never reach a concentration high enough to be directly detected. To this aim, the use of selected compounds, called spin-trapping agents, is of crucial importance. The spin-trapping agents react with the mentioned transient reactive species to yield stabilized radicals to be detected and measured via EPR spectroscopy. Most of the spin-trapping agents have a nitron-type group, which forms a nitroxide (spin adduct) during the trapping of the free radical. Among several nitrones used as spin traps, N-tert-butyl- $\alpha$ -phenylnitron (PBN) was preferred due to its lipophilic character and stability of the resulting spin adducts [19]. Furthermore, PBN was successfully used as a spin-trapping agent to evaluate lipid free radicals in food lipids [20], edible vegetable oils, and their mixtures [21].

The objective of this study was to assess the possibility of employing EPR spectroscopy coupled with the spin trapping technique to determine the oxidative stability of vegetable oils. The employment of such a method could constitute a valid alternative to the conventional techniques employed both to compare different materials and to evaluate the stability of the final cosmetic products under various conditions. As a proof of concept, the oxidative stability of extra virgin olive oil (EVOO), sweet almond oil (SAO), apricot kernel oil (AKO), and Jojoba oil (JO) was evaluated by monitoring the free radical formation following UV irradiation by using the EPR spin trapping technique.

## 2. Materials and Methods

### 2.1. Chemicals

N-tert-Butyl- $\alpha$ -phenylnitron (PBN) (purity 97%) was obtained from Sigma-Aldrich Merck KGaA, (Darmstadt, Germany).

### 2.2. Samples

EVOO was provided by Agricultural Cooperatives of Castelvetro (Sicily, Italy). AKO (Erboristeria Magentina, Poirino (TO) Italy), SAO, and JO (Marco Viti S.p.A., Vicenza, Italy) were of pharmaceutical grade (according to European Pharmacopoeia) and purchased from a local pharmacy.

### 2.3. UV Irradiation of Oils

A carefully weighted aliquot of oil ( $1.00 \pm 0.05$  g) was spread on a  $5 \times 5$  cm glass plate which was then placed on a plastic black box at a distance of 20 cm from the light source. A commercial UVA LED lamp (wavelength range: 315–400 nm; power: 50 W; Philips, Groningen, The Netherlands) was used for irradiation. The samples were irradiated for 30, 60, and 120 min. Each experiment was performed twice ( $n = 2$ ).

### 2.4. Treatment with the Spin-Trapping Agent

To assess the formation of free radicals following UV irradiation and to predict the oxidative stability of the examined oils, a literature method was employed and just slightly modified [22]. Briefly, 3 mg of PBN were dissolved in 1 g of each irradiated oil via stirring. Afterwards, three aliquots of each oil sample were put in ESR tubes (710-SQ; Wilmad LabGlass, Vineland, NJ, USA) and placed in a water bath at  $70^\circ\text{C}$  in the dark for increasing incubation times (from a minimum of 5 to a maximum of 180 min). At each time point, each tube was then equilibrated in a water bath at  $25^\circ\text{C}$  and subjected to EPR analyses, as described below. Then, the tubes were placed again at  $70^\circ\text{C}$  until reaching the next time point. The same procedure was conducted on each not-irradiated oil. The treatment with the spin-trapping agent was performed twice ( $n = 2$ ).

### 2.5. EPR Measurements

The EPR measurements were carried out on both not-irradiated and irradiated oils at constant room temperature ( $25^\circ\text{C}$ ), using an e-scan Food Analyzer EPR spectrometer (Bruker, Rheinstetten, Germany) operating at the X-band. The parameters used in all EPR measurements were the following: microwave power, 3 mW; modulation amplitude, 5.0 G; modulation frequency, 75 kHz; conversion time, 41 ms. Each sample previously treated with PBN was incubated at  $70^\circ\text{C}$  for 5 min, then equilibrated at  $25^\circ\text{C}$  for 2–3 min, and then subjected to the EPR measurement (3 min approximately). The same sample was then incubated again at  $70^\circ\text{C}$  for a further 5 min, and the procedure was repeated up to a total thermic treatment of 180 min. Thus, the measurements were carried out after multiple 5 min treatments. Each measurement was repeated three times and results are reported as means ( $n = 6$ )  $\pm$  SD.

### 2.6. Manipulation of the EPR Spectra

To compare the experimental results the following parameters were considered:

- $H_{p/p}$ : the peak-to-peak amplitude measured considering the first peak of the PBN-adduct signal obtained after every tested incubation time at  $70^\circ\text{C}$ ;
- Induction time (IT) or induction period (IP): the lag-time corresponding to a period of time during which radicals are formed very slowly. It is followed by a sudden sharp linear increase in radical production. This value is equal to the projection on the x axis of the point of intersection between the tangents to the two portions of the bimodal curve obtained when plotting the  $H_{p/p}$  as a function of incubation time at  $70^\circ\text{C}$ ;
- The slope of the linear portion of the curve obtained by plotting the  $H_{p/p}$  as a function of incubation time at  $70^\circ\text{C}$ .

### 2.7. Statistical Analysis

The data are expressed as mean  $\pm$  standard deviation (SD). All differences were statistically evaluated with the Student's *t* test or the one-way analysis of variance (ANOVA or F-test) with the minimum levels of significance set at  $p < 0.05$ .

## 3. Results

The most popular anti-aging treatments contain antioxidants which can act directly by restoring the physiological radical balance and/or indirectly by preventing the photoaging process. Vitamins and phenols are some of the most representative examples of cosmetic active ingredients used for anti-aging purposes. They can be used both as pure

components or by carefully selecting precious vegetable oils characterized by a relevant and rich antioxidant unsaponifiable fraction. According to their composition (Table 1), EVOO, SAO, AKO, and JO certainly possess several compounds which could be responsible for their antioxidant properties and oxidative stability [16,17,23,24]. Despite their extreme variability in composition, depending on the cultivars, the harvest time, and also on the analytical methods employed [25], these characteristics make them widely used vegetable oils of cosmetic interest. Consequently, samples were examined in terms of free radical production via the EPR spin trapping technique using PBN coupled with thermal treatment at 70 °C.

**Table 1.** Quali-quantitative composition of EVOO, AKO, SAO, and JO.

	EVOO [23]	SAO [16]	AKO [24]	JO * [17]
<b>Fatty Acids (<i>w/w</i>%)</b>				
<b>MUFAs</b>	e.g., oleic acid: 55–83%	e.g., oleic acid: 65%	e.g., oleic acid: 60–71%	e.g., oleic acid: 10%; 11-eicosenoic acid: 70%;
<b>PUFAs</b>	e.g., linoleic acid: 4–20%	e.g., linoleic acid: 37%	e.g., linoleic acid: 20–23%	
<b>SFAs</b>	e.g., palmitic acid: 7.5–20%;	e.g., palmitic acid: 9%; stearic acid: 3%	e.g., palmitic acid: 2.9–3.4%;	e.g., palmitic acid: 1.2%; stearic acid: 0.1%
<b>Unsaponifiable fraction</b>				
<b>Tocopherols</b>	97–785 mg/kg e.g., $\alpha$ -tocopherol: 100–330 mg/kg	e.g., $\alpha$ -tocopherol: 20 mg/kg; $\beta$ -tocopherol: 2 mg/kg; $\gamma$ -tocopherol: 5 mg/kg	e.g., $\alpha$ -tocopherol: 14.8–40.4 mg/kg; $\gamma$ -tocopherol: 330.8–520.8 mg/kg; $\delta$ -tocopherol: 28.5–60.2 mg/kg	e.g., $\gamma$ -tocopherol 79%
<b>Phenols (TPC)</b>	50–800 mg/kg e.g., Tyrosol, hydroxytyrosol, and secoiridoids: c.a. 90%; lignans: c.a. 10%			
<b>Pigments</b>	1–20 mg/kg		e.g., $\beta$ -carotene: 57.2 $\mu$ g/g	
<b>Hydrocarbons</b>	200–7500 mg/kg	e.g., squalene: 100 $\mu$ g/g		
<b>Waxes</b>				e.g., Docosenyl eicosenoate 41% Eicosenyl eicosenoate: 28%

MUFAs: Mono-Unsaturated Fatty Acids; PUFAs: Poly-Unsaturated Fatty Acids; SFAs: Saturated Fatty Acids.  
\* JO is composed of almost 98% pure waxes (wax esters, free acids, free alcohols, and hydrocarbons), sterols, and vitamins with few triglyceride esters; so, it is widely known as liquid wax rather than oil. It also contains other fat-soluble vitamins such as vitamin A [17].

Firstly, the EPR spectra of each oil (not irradiated or irradiated for different periods of time) were acquired following the treatment with a fixed amount of PBN but a different period of thermal treatment (70 °C). As an example, Figure 1 shows the EPR spectra of the stable PBN spin adducts formed in the EVOO sample after 30 min of incubation at 70 °C with the not-irradiated sample and UV-irradiated ones (30, 60, and 120 min). As is observable, the intensity of the EPR signal increases together with the UV irradiation time. This increase is indicative of PBN spin adducts' accumulation, corresponding to greater free radical production. Similar results have been obtained for the other analyzed oils.

Clearly, the PBN-adducts formation measurable via EPR spectroscopy is strictly connected to the formation of free radicals caused by the UV irradiation treatment and/or the following thermal incubation period. This phenomenon was then monitored by measuring the peak-to-peak amplitude ( $H_{p/p}$ ) between the EPR signals of the PBN-adduct (as shown in Figure 1) every 5 min of thermal treatment at 70 °C. It should be noted that, also immediately after irradiation, the signal was not equal to 0. Indeed, the ratio of the EPR signal of all oils after UV irradiation vs. unirradiated is in the range 1.5–12. To compare and analyze the enormous set of obtained data, the calculated  $H_{p/p}$  values were plotted against time to highlight the accumulation of free radicals. Furthermore, according to several studies aimed at predicting the oxidative stability of oils [21,22,26], the obtained graphs were used to determine both the induction time and the slope of the linear portion. The induction time (IT), also called the induction period (IP) or lag-time, corresponds to the range of time during which radicals are formed very slowly before a sudden sharp linear appears. It is, therefore, an index of the oxidative stability of each sample, and it is equal to the projection on the x axis of the point of intersection between the tangents to the two portions of the

bimodal curve obtained when plotting the  $H_{p/p}$  as a function of incubation time at 70 °C. Figure 2 is reported as a representative example of IT determination.

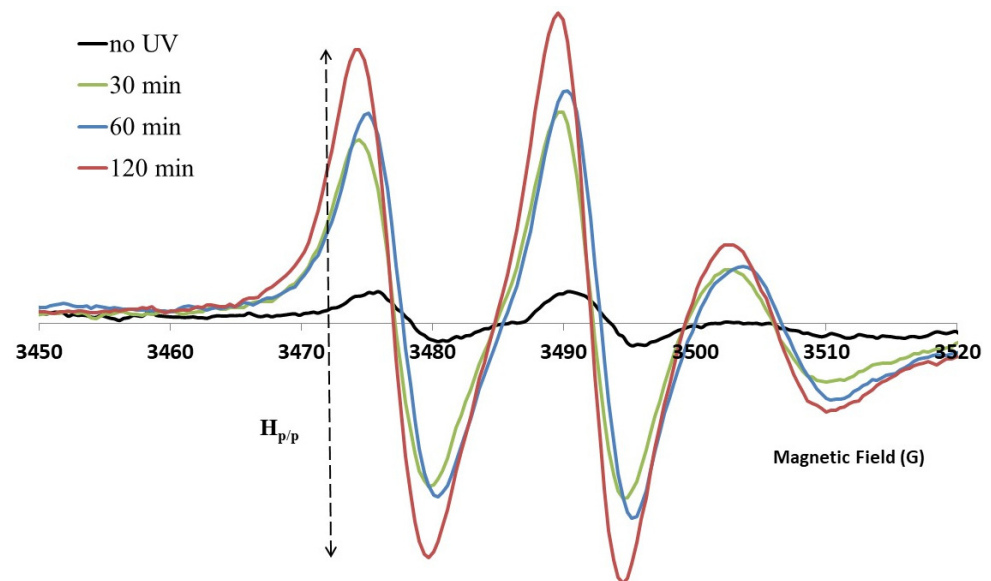


**Figure 1.** EPR spectra of the PBN spin adducts in EVOO after 30 min of incubation at 70 °C with the not-irradiated (black line) sample and UV-irradiated ones (30 min: green line; 60 min: blue line; 120 min: red line). Results are reported as means ( $n = 6$ ).

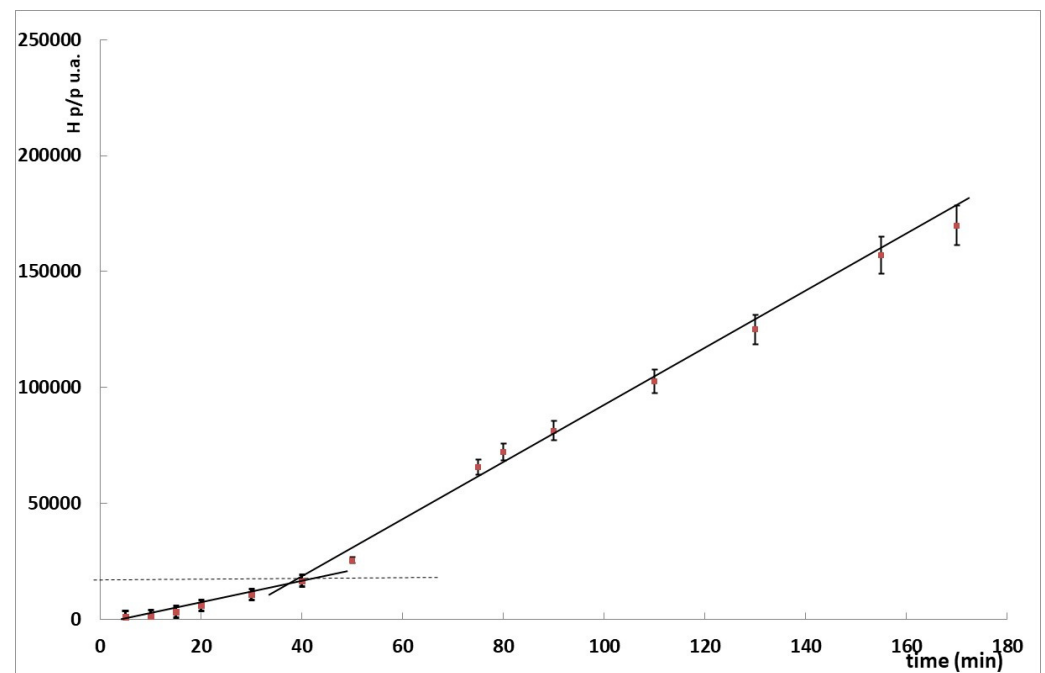


**Figure 2.** Determination of the induction time (IT) for EVOO (sample not irradiated). Results are reported as means ( $n = 6$ ).

The IT values for all the tested samples are reported in Table 2.

Higher IT values correspond to enhanced oxidative resistance and thus reduced free radical formation; conversely, smaller IT values indicated the susceptibility to free radical formation and, therefore, reduced oxidative stability of the oil. As reported in Table 2, the IT values calculated for not-irradiated oils suggest that EVOO and JO are more resistant to the formation of free radicals than ASO and AKO. Following the UV irradiation, the IT

values decrease almost proportionally with irradiation time for all the analyzed oils. Again, EVOO and JO turn out to be the most powerful in terms of antioxidant properties as they displayed the greater IT values after 120 min of UV irradiation. These results indicate that during the UV irradiation treatment, the natural antioxidant agents contained in EVOO and JO samples were more powerful than the AKO and SAO ones, thus not yet being exhausted after 120 min of UV treatment.

**Table 2.** IT values determined via EPR spectroscopy for EVOO, SAO, AKO, and JO both when not irradiated and UV irradiated for 30, 60, and 120 min.

Sample	No UV	30 min UV	60 min UV	120 min UV
EVOO	40 min	20 min	10 min	7 min
SAO	20 min	10 min	10 min	5 min
AKO	25 min	15 min	10 min	5 min
JO	50 min	35 min	20 min	15 min

The slope of the linear portion of the signals as a function of incubation time after the IT could be a simple way to measure the oxidative stability in later stages, when the depletion of oil's antioxidants is happening.

In order to confirm the obtained results, the slope of the linear portion of the graphs obtained by plotting the  $H_{p/p}$  values as a function of incubation time at 70° were evaluated. First of all, to better discuss and visualize the obtained data, each tested oil will be reported by itself.

The behavior of EVOO samples is depicted in Figure 3.

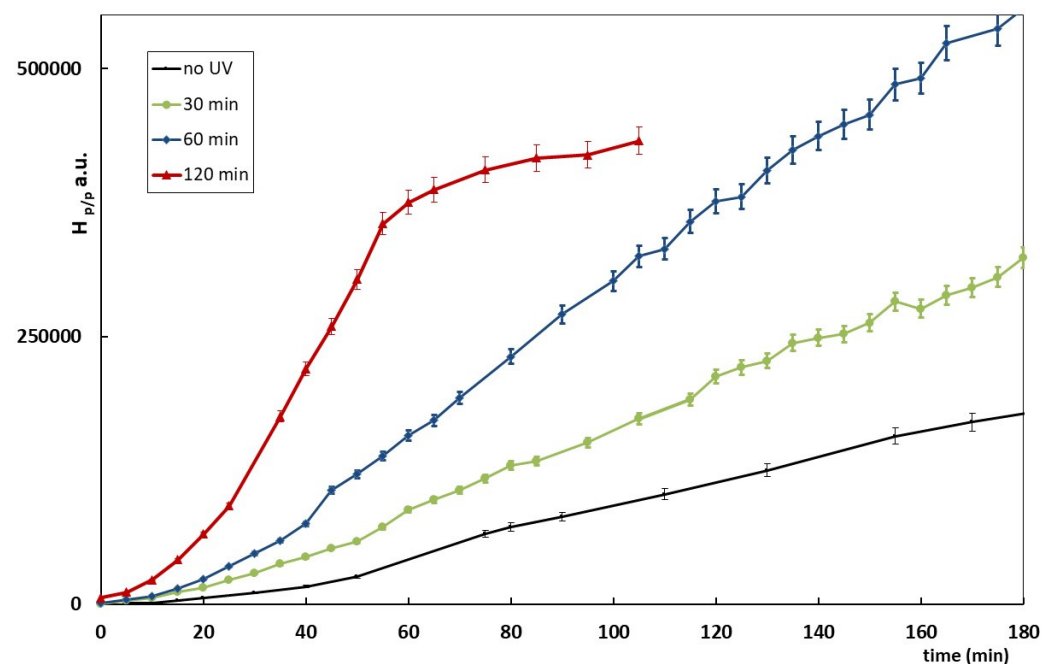


**Figure 3.**  $H_{p/p}$  intensity against incubation time at 70 °C for EVOO samples. Means (n = 6)  $\pm$  SD.

As reported, a sharp linear increase in the  $H_{p/p}$  intensity during storage at 70 °C is observable, and it is clearly visible that the slopes of the curves increase by increasing the irradiation time; thus, the greatest slope corresponds to the EVOO sample subjected to 120 min of UV irradiation. This sample also evolves, after 55 min of incubation at 70 °C, into an abrupt change in slope, which became similar to a quasi-plateau phase and also resembles the slope of the not-irradiated sample, indicating a slow production of free radicals after antioxidants depletion. For samples not irradiated and UV irradiated for 30 and 60 min, the experimental results relating to the time interval between IT and 180 min were selected as the linear portion, while, for samples irradiated for 120 min,

the considered linear portion was the one located between the IT and the quasi-plateau phase. The experimental data were fitted with a straight-line equation, and the slopes obtained from the best-fit line are reported in Table 3. As reported, the slope of the obtained straight line resulted as 6.6 times higher for the 120 min irradiated sample compared to the not-irradiated one. The increase in slope by increasing the time of UV irradiation corresponds to the reaction of the antioxidant agents present in high levels in EVOO oil, such as  $\alpha$ -tocopherol,  $\beta$ -carotene, squalene, phenols, and unsaturated fatty acids such as oleic and linoleic acids. The quasi-plateau phase corresponds to the exhaustion of these agents without further alteration of the lipidic matrix.

**Table 3.** Best-fit line ( $R > 0.99$ ) equation for the linear portion for the  $H_{p/p}$  intensity against incubation time at 70 °C graphs obtained for EVOO samples both not irradiated and UV irradiated for 30, 60, and 120 min.

EVOO	Best-Fit Line Equation	$R^2$	Linearity Time Range (min)
No UV	$y = 1203x - 28,642$	0.9919	45–180
30 min UV	$y = 1962x - 31,321$	0.9976	25–180
60 min UV	$y = 3387x - 45,103$	0.9972	15–180
120 min UV	$y = 7930x - 31,321$	0.9926	10–55

The behavior of SAO samples is depicted in Figure 4.

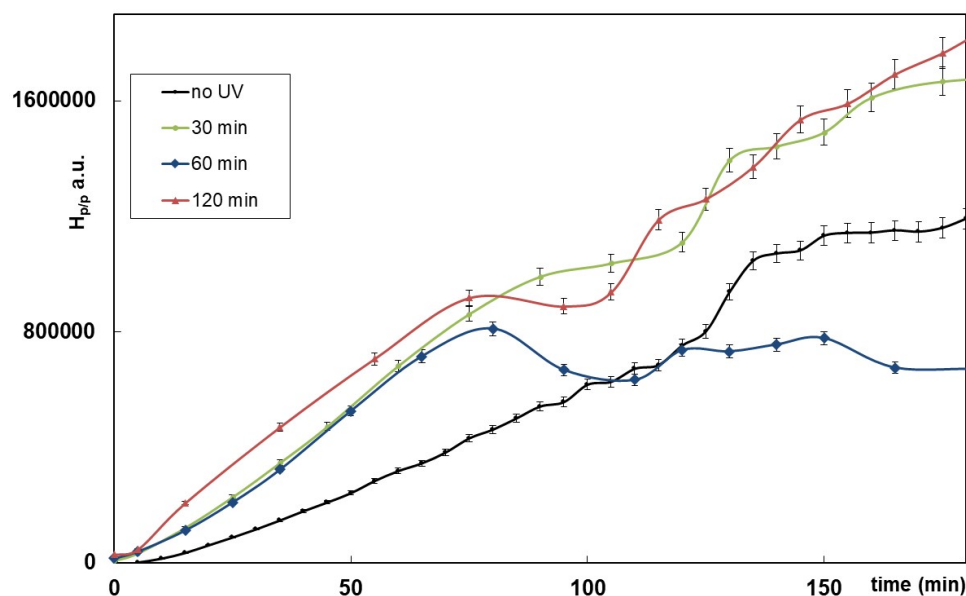


**Figure 4.**  $H_{p/p}$  intensity against incubation time at 70 °C for SAO samples. Means ( $n = 6$ )  $\pm$  SD.

As reported, for the not-irradiated sample, the  $H_{p/p}$  intensity linearly increases with incubation time up to 120 min, after a plateau phase is observed. The samples irradiated for 30 and 60 min showed a similar initial linear trend up to 90 and 80 min, respectively. This linear region is followed by a continuous  $H_{p/p}$  increase which is not linear. The behavior of the 120 min irradiated samples starts analogously, highlighting a linear trend until 75 min. The experimental data were fitted with a straight-line equation, and the slopes obtained from the best-fit line are reported in Table 4. As reported, the slope of the obtained straight line is doubled for the irradiated samples (a not-significant variation was observed between these samples) respect the not irradiated one. The different time-dependent profiles can be related to the different antioxidants contained in the SAO sample and modified by both the UV irradiation and the further incubation at 70 °C. The unique behavior of SAO, characterized by a fluctuating trend of rises and falls for the irradiated samples otherwise not observed in the non-irradiated one, could be related to the presence

of several tocopherol isoforms ( $\alpha$ ,  $\gamma$ , and  $\delta$ ; see Table 1) which differently absorb the energy from UV radiation, thus becoming radicals able to bind to the PBN and undergoing depletion independently and not in synchrony.

**Table 4.** Best-fit line ( $R > 0.99$ ) equation for the linear portion for the  $H_{p/p}$  intensity against incubation time at 70 °C graphs obtained for SAO samples both not irradiated and UV irradiated for 30, 60, and 120 min.

SAO	Best-Fit Line Equation	$R^2$	Linearity Time Range (min)
No UV	$y = 6036x - 6234$	0.9992	25–120
30 min UV	$y = 12,464x - 79,252$	0.9968	15–90
60 min UV	$y = 12,236x - 87,839$	0.9969	15–80
120 min UV	$y = 12,683x + 11,144$	0.9926	10–75

The behavior of AKO samples is depicted in Figure 5.

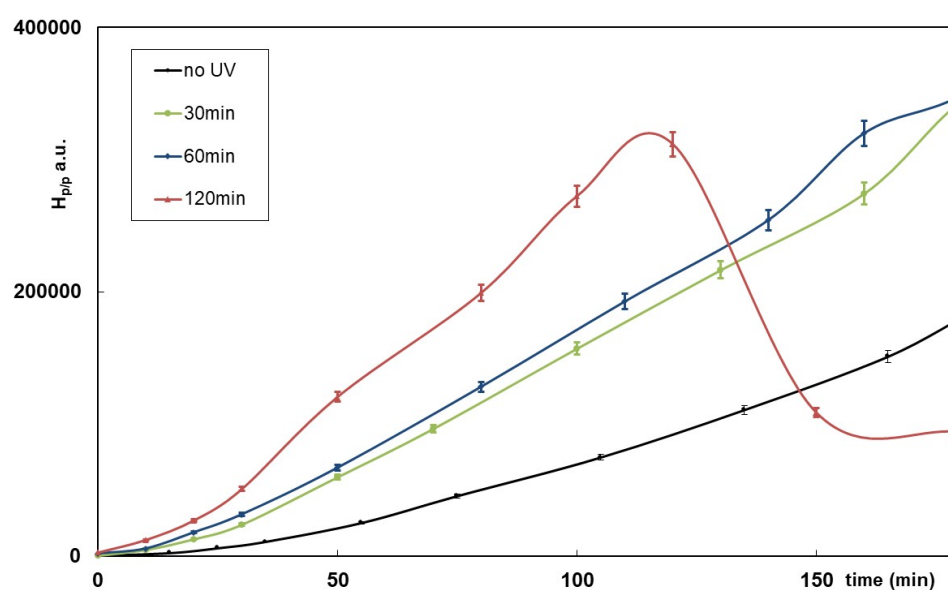


**Figure 5.**  $H_{p/p}$  intensity against incubation time at 70 °C for AKO samples. Means ( $n = 6$ )  $\pm$  SD.

The AKO not-irradiated sample showed a linear trend from the IT to 180 min. The slopes of straight lines obtained for samples irradiated for 30 and 60 min were not significantly different. In contrast, for the 120 min irradiated sample, after about 110 min of thermal incubation, the  $H_{p/p}$  intensity quickly decreases, due to alteration of the lipid matrix following exhaustion of the antioxidant components. The experimental data were fitted with a straight-line equation, and the slopes obtained from the best-fit line are reported in Table 5. As reported, the slope of the obtained straight line is 2.3-times higher for the 120 min irradiated sample compared to the not-irradiated one.

**Table 5.** Best-fit line ( $R > 0.99$ ) equation for the linear portion for the  $H_{p/p}$  intensity against incubation time at 70 °C graphs obtained for SAO samples both not irradiated and UV irradiated for 30, 60, and 120 min.

AKO	Best-Fit Line Equation	$R^2$	Linearity Time Range (min)
No UV	$y = 1338x - 6234$	0.9936	25–180
30 min UV	$y = 1965x - 34,686$	0.9954	35–180
60 min UV	$y = 2003x - 87,839$	0.9964	15–180
120 min UV	$y = 3040x + 11,144$	0.9970	20–100

Finally, the behavior of JO samples is depicted in Figure 6.



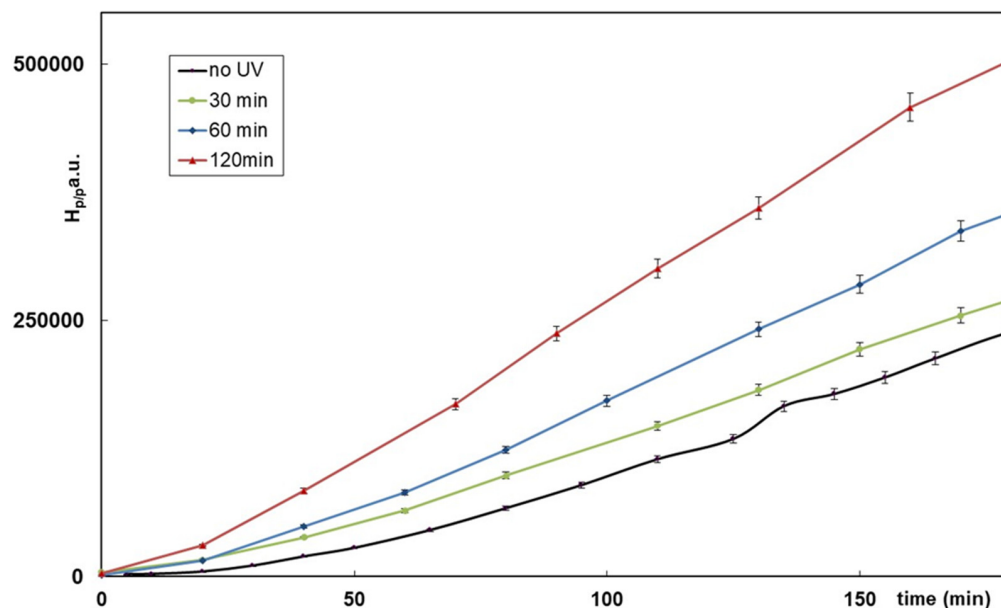


**Figure 6.**  $H_{p/p}$  intensity against incubation time at 70 °C for JO samples. Means ( $n = 6$ )  $\pm$  SD.

As reported, a sharp linear increase in the  $H_{p/p}$  intensity during storage at 70 °C as observed for all the studied samples; no plateau phase or intensity reduction were found after 120 min of UV irradiation. The experimental data were fitted with a straight-line equation, and the slopes obtained from the best-fit line are reported in Table 6. As reported, the slope of the obtained straight line is less than doubled for the 120 min irradiated sample compared to the not-irradiated one. Furthermore, for all the JO samples, the linearity region went from the IT to 180 min. This phenomenon could be attributed to the composition of JO which is almost 98% pure waxes and antioxidants ( $\alpha$ ,  $\gamma$ , and  $\delta$  tocopherol) which confer high thermal and oxidative stabilities.

**Table 6.** Best-fit line ( $R > 0.99$ ) equation for the linear portion for the  $H_{p/p}$  intensity against incubation time at 70 °C graphs obtained for SAO samples both not irradiated and UV irradiated for 30, 60, and 120 min.

JO	Best-Fit Line Equation	$R^2$	Linearity Time Range (min)
No UV	$y = 1535x - 6234$	0.9949	50–180
30 min UV	$y = 1715x - 38,985$	0.9992	35–180
60 min UV	$y = 2227x - 87,839$	0.9983	25–180
120 min UV	$y = 2940x + 28,732$	0.9970	20–100

To further highlight and compare the behavior of the four studied oils, the calculated slope of the linearity regions previously discussed were plotted as a function of the UV irradiation time. As depicted in Figure 7, AKO and JO samples displayed a similar behavior characterized by a slope increase proportional to the UV irradiation time. The trend for the EVOO sample showed, instead, an exponential behavior. While, finally, the SAO behavior was not curve fitted with any simple equation as the slope just doubled following UV irradiation, but it was independent of the exposure time.

To summarize, by considering all the information acquired through EPR spectroscopy, the following considerations can be made regarding the four tested vegetable oils:

- JO possesses the highest antioxidant properties as, in the absence of UV irradiation treatment, it has the highest calculated IT (50 min). Additionally, it also possesses the greatest oxidative stability, as following the maximum tested UV irradiation time (120 min) the IT value is reduced to only a third of the initial value (from 50 to 15 min) while the same value is 4-, 5-, and 5.7-fold reduced for the AKO, SAO, and EVOO samples, respectively;

- AKO starts as less powerful but seems to be quite stable to oxidation overtime. However, it should be noted that following 120 min of UV irradiation, the thermal treatment caused the alteration of the lipid matrix thus compromising the physical and chemical stability of this oil and consequently of the hypothetical cosmetic product in which it should be inserted;
- EVOO possesses high antioxidant properties but low oxidative stability, as highlighted from the exponential behavior depicted in Figure 7;
- SAO is the least stable tested oil with respect to oxidation, as after just 30 min of UV irradiation the  $H_{p/p}$  values determined are close the maximum obtained (120 min UV irradiation).

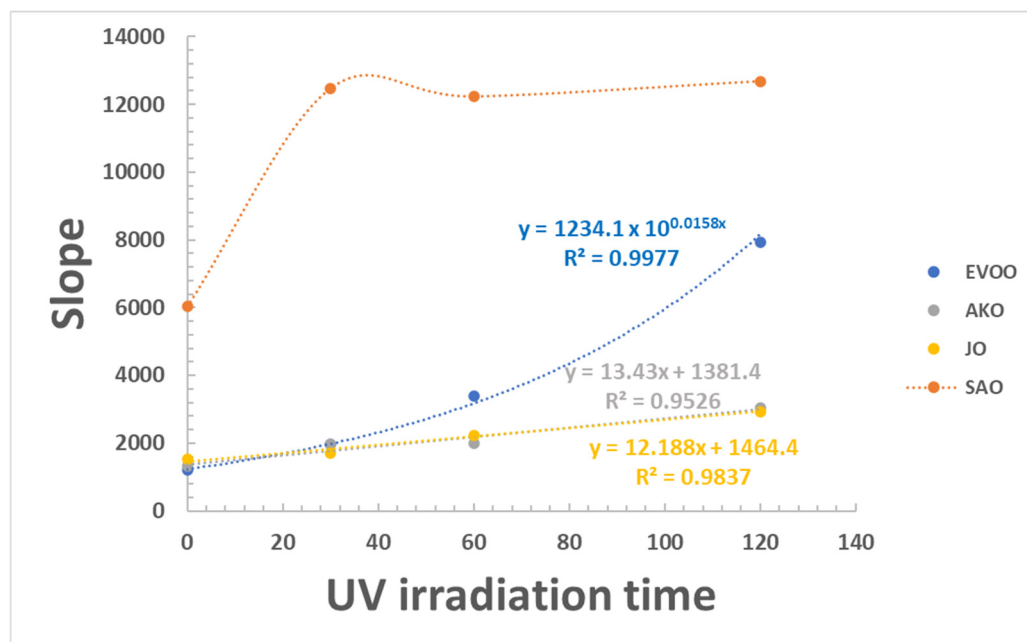


**Figure 7.** Slope of the linear portion of the  $H_{p/p}$  intensity against incubation time at 70 °C graphs as a function of UV irradiation time for EVOO, SAO, AKO, and JO samples. Means (n = 6).

#### 4. Conclusions

EPR spectroscopy coupled with the spin trapping technique could provide relevant information regarding the antioxidant power and the oxidative stability of vegetable oils, thus being a valid alternative to the other well-known methodologies (e.g., DPPH, ORAC, and ABTS assays) used to assess these activities and compare different raw materials. The knowledge that can be acquired through this technique can be used for several purposes: (i) compare different vegetable oils and (ii) evaluate the oxidative stability of the final cosmetic product under the possible usage conditions. The anti-aging products are generally classified also into “day” and “night” products. Indeed, e.g., to develop a “day” anti-aging product, the use of vegetable oils characterized by high content of natural antioxidants but low oxidative stability to both light and temperature would not be successful in determining the direct anti-aging effect as the administered dose of active molecules will not be available to perform its action. In contrast, the interaction with the UV radiation could be useful in preventing photoaging. However, in this regard, some other questions should be addressed, e.g., regarding the safety of the production of extremely reactive radicals which could lead to the development of an undesirable radical cascade. It is worth noting that the here-proposed methodology can further be modified and “adjusted” to achieve different results. For example, by varying the UV source, the methodology still remains the same: with UVB radiation as the main reason for photoaging via this methodology, it could be attributed to the “photoaging preventive” claim to a cosmetic product based on the oil content. Moreover, considering that UVB radiation has higher energy than the UVA one,

and that the proposed technique allows for detecting differences in oils' behaviors when subjected to UVA treatment, the here-reported methodology will certainly also work when subjecting samples to a higher-energy treatment. Finally, it should be emphasized that these first encouraging results can act as the starting point to further develop a quantitative method based on the EPR analyses in order to achieve comparable quantitative results from this innovative approach and the already-cited most common ones.

**Author Contributions:** Conceptualization, M.C.D. and V.D.C.; methodology, M.C.D.; formal analysis, C.C. and G.O.; investigation, M.C.D.; resources, C.C. and G.O.; data curation, M.C.D., G.D.P. and V.D.C.; writing—original draft preparation, M.C.D.; writing—review and editing, G.D.P. and V.D.C.; funding acquisition, M.C.D., G.D.P. and V.D.C. All authors have read and agreed to the published version of the manuscript.

**Funding:** This work was supported by grants from the University of Palermo (grant number FFR-D15-008633, FFR-D15-502204, FFR-D15-160695).

**Institutional Review Board Statement:** Not applicable.

**Informed Consent Statement:** Not applicable.

**Data Availability Statement:** The original contributions presented in the study are included in the article, further inquiries can be directed to the corresponding author.

**Acknowledgments:** Agricultural Cooperatives of Castelvetrano (Sicily, Italy) which kindly supplied EVOO.

**Conflicts of Interest:** The authors declare no conflicts of interest.

## References

1. Fisher, G.J.; Kang, S.; Varani, J.; Bata-Csorgo, Z.; Wan, Y.; Datta, S.; Voorhees, J.J. Mechanisms of Photoaging and Chronological Skin Aging. *Arch. Dermatol.* **2002**, *138*, 1462–1470. [[CrossRef](#)]
2. Rittie, L.; Fisher, G.J. Natural and Sun-Induced Aging of Human Skin. *Cold Spring Harb. Perspect. Med.* **2015**, *5*, a015370. [[CrossRef](#)] [[PubMed](#)]
3. He, X.; Wan, F.; Su, W.; Xie, W. Research Progress on Skin Aging and Active Ingredients. *Molecules* **2023**, *28*, 5556. [[CrossRef](#)] [[PubMed](#)]
4. Burke, K.E. Photoprotection of the Skin with Vitamins C and E: Antioxidants and Synergies. In *Nutrition and Skin*; Pappas, A., Ed.; Springer: New York, NY, USA, 2011; pp. 43–58, ISBN 978-1-4419-7967-4.
5. Pinnell, S.R. Cutaneous Photodamage, Oxidative Stress, and Topical Antioxidant Protection. *J. Am. Acad. Dermatol.* **2003**, *48*, 1–19. [[CrossRef](#)] [[PubMed](#)]
6. Nichols, J.A.; Katiyar, S.K. Skin Photoprotection by Natural Polyphenols: Anti-Inflammatory, Antioxidant and DNA Repair Mechanisms. *Arch. Dermatol. Res.* **2010**, *302*, 71–83. [[CrossRef](#)] [[PubMed](#)]
7. Lee, J.H.; Park, J.; Shin, D.W. The Molecular Mechanism of Polyphenols with Anti-Aging Activity in Aged Human Dermal Fibroblasts. *Molecules* **2022**, *27*, 4351. [[CrossRef](#)]
8. Angellotti, G.; Di Prima, G.; D'Agostino, F.; Peri, E.; Tricoli, M.R.; Belfiore, E.; Allegra, M.; Cancemi, P.; De Caro, V. Multicomponent Antibiofilm Lipid Nanoparticles as Novel Platform to Ameliorate Resveratrol Properties: Preliminary Outcomes on Fibroblast Proliferation and Migration. *Int. J. Mol. Sci.* **2023**, *24*, 8382. [[CrossRef](#)]
9. Dunaway, S.; Odin, R.; Zhou, L.; Ji, L.; Zhang, Y.; Kadekaro, A.L. Natural Antioxidants: Multiple Mechanisms to Protect Skin From Solar Radiation. *Front. Pharmacol.* **2018**, *9*, 392. [[CrossRef](#)]
10. Di Prima, G.; Belfiore, E.; Migliore, M.; Scarpaci, A.G.; Angellotti, G.; Restivo, I.; Allegra, M.; Arizza, V.; De Caro, V. Green Extraction of Polyphenols from Waste Bentonite to Produce Functional Antioxidant Excipients for Cosmetic and Pharmaceutical Purposes: A Waste-to-Market Approach. *Antioxidants* **2022**, *11*, 2493. [[CrossRef](#)]
11. Di Prima, G.; Belfiore, E.; Angellotti, G.; De Caro, V. Green Next-Generation Excipients Enriched in Polyphenols from Recovery of Grape Processing Waste Black Bentonite: Influence of Unconventional Extraction Solvents on Antioxidant Properties and Composition. *Sustain. Chem. Pharm.* **2024**, *37*, 101414. [[CrossRef](#)]
12. Klaschka, U. Natural Personal Care Products—Analysis of Ingredient Lists and Legal Situation. *Environ. Sci. Eur.* **2016**, *28*, 8. [[CrossRef](#)] [[PubMed](#)]
13. Moskwa, J.; Bronikowska, M.; Socha, K.; Markiewicz-Żukowska, R. Vegetable as a Source of Bioactive Compounds with Photoprotective Properties: Implication in the Aging Process. *Nutrients* **2023**, *15*, 3594. [[CrossRef](#)] [[PubMed](#)]
14. Jimenez-Lopez, C.; Carpena, M.; Lourenço-Lopes, C.; Gallardo-Gomez, M.; Lorenzo, J.M.; Barba, F.J.; Prieto, M.A.; Simal-Gandara, J. Bioactive Compounds and Quality of Extra Virgin Olive Oil. *Foods* **2020**, *9*, 1014. [[CrossRef](#)] [[PubMed](#)]

15. Lino, C.; Bongiorno, D.; Pitzonzo, R.; Indelicato, S.; Barbera, M.; Di Gregorio, G.; Pane, D.; Avellone, G. Chemical Characterization, Stability and Sensory Evaluation of Sicilian Extra Virgin Olive Oils: Healthiness Evidence at Nose Reach. *Foods* **2024**, *13*, 2149. [[CrossRef](#)]
16. Ouzir, M.; El Bernoussi, S.; Tabyaoui, M.; Taghzouti, K. Almond Oil: A Comprehensive Review of Chemical Composition, Extraction Methods, Preservation Conditions, Potential Health Benefits, and Safety. *Compr. Rev. Food Sci. Food Saf.* **2021**, *20*, 3344–3387. [[CrossRef](#)]
17. Gad, H.A.; Roberts, A.; Hamzi, S.H.; Gad, H.A.; Touiss, I.; Altyar, A.E.; Kensara, O.A.; Ashour, M.L. Jojoba Oil: An Updated Comprehensive Review on Chemistry, Pharmaceutical Uses, and Toxicity. *Polymers* **2021**, *13*, 1711. [[CrossRef](#)]
18. D'Oca, M.C.; Bartolotta, A. Evaluation of the Original Dose in Irradiated Dried Fruit by EPR Spectroscopy. *Radiat. Meas.* **2011**, *46*, 813–815. [[CrossRef](#)]
19. Thomsen, M.K.; Kristensen, D.; Skibsted, L.H. Electron Spin Resonance Spectroscopy for Determination of the Oxidative Stability of Food Lipids. *J. Am. Oil Chem. Soc.* **2000**, *77*, 725–730. [[CrossRef](#)]
20. Thomsen, M.K.; Vedstesen, H.; Skibsted, L.H. Quantification of Radical Formation in Oil-in-water Food Emulsions by Electron Spin Resonance Spectroscopy. *J. Food Lipids* **1999**, *6*, 149–158. [[CrossRef](#)]
21. Velasco, J.; Andersen, M.L.; Skibsted, L.H. Evaluation of Oxidative Stability of Vegetable Oils by Monitoring the Tendency to Radical Formation. A Comparison of Electron Spin Resonance Spectroscopy with the Rancimat Method and Differential Scanning Calorimetry. *Food Chem.* **2004**, *85*, 623–632. [[CrossRef](#)]
22. Papadimitriou, V.; Sotiroidis, T.G.; Xenakis, A.; Sofikiti, N.; Stavviannoudaki, V.; Chaniotakis, N. Oxidative Stability and Radical Scavenging Activity of Extra Virgin Olive Oils: An Electron Paramagnetic Resonance Spectroscopy Study. *Anal. Chim. Acta* **2006**, *573–574*, 453–458. [[CrossRef](#)] [[PubMed](#)]
23. Capurso, A.; Crepaldi, G.; Capurso, C. Extra-Virgin Olive Oil (EVOO): History and Chemical Composition. In *Benefits of the Mediterranean Diet in the Elderly Patient. Practical Issues in Geriatrics*; Capurso, A., Crepaldi, G., Capurso, C., Eds.; Springer International Publishing: Cham, Switzerland, 2018; pp. 11–21, ISBN 978-3-319-78084-9.
24. Stryjecka, M.; Kieltyka-Dadasiewicz, A.; Michalak, M.; Rachoń, L.; Głowacka, A. Chemical Composition and Antioxidant Properties of Oils from the Seeds of Five Apricot (*Prunus armeniaca* L.) Cultivars. *J. Oleo Sci.* **2019**, *68*, 729–738. [[CrossRef](#)] [[PubMed](#)]
25. Bongiorno, D.; Di Stefano, V.; Indelicato, S.; Avellone, G.; Ceraulo, L. Bio-phenols Determination in Olive Oils: Recent Mass Spectrometry Approaches. *Mass Spectrom. Rev.* **2023**, *42*, 1462–1502. [[CrossRef](#)] [[PubMed](#)]
26. Fadda, A.; Molinu, M.G.; Deiana, P.; Sanna, D. Electron Paramagnetic Resonance Spin Trapping of Sunflower and Olive Oils Subjected to Thermal Treatment: Optimization of Experimental and Fitting Parameters. *ACS Food Sci. Technol.* **2021**, *1*, 1294–1303. [[CrossRef](#)]

**Disclaimer/Publisher's Note:** The statements, opinions and data contained in all publications are solely those of the individual author(s) and contributor(s) and not of MDPI and/or the editor(s). MDPI and/or the editor(s) disclaim responsibility for any injury to people or property resulting from any ideas, methods, instructions or products referred to in the content.